Water Research 219 (2022) 118457

Contents lists available at ScienceDirect

Water Research

journal homepage: www.elsevier.com/locate/watres

UV/Sodium percarbonate for bisphenol A treatment in water: Impact of water quality parameters on the formation of reactive radicals

Jiong Gao [a], Roberta Frinhani Nunes [b], Kevin O'Shea [c], Greg L. Saylor [a], Lingjun Bu [d], Yu-Gyeong Kang [a], Xiaodi Duan [e,*], Dionysios D. Dionysiou [a,*], Shenglian Luo [f]

[a] Environmental Engineering and Science Program, Department of Chemical and Environmental Engineering, University of Cincinnati, Cincinnati, OH 45221, USA
[b] Department of Chemical Engineering, Escola Politécnica, University of São Paulo, tr. 3, São Paulo 380, Brazil
[c] Department of Chemistry and Biochemistry, Florida International University, Miami, FL 33199, USA
[d] Department of Water Engineering and Science, Hunan University, Hunan, Changsha 410082, China
[e] Key Laboratory of Organic Compound Pollution Control Engineering (MOE), School of Environmental and Chemical Engineering, Shanghai University, Shanghai 200444, China
[f] College of Environmental and Chemical Engineering, Nanchang Hangkong University, Nanchang, Jiangxi 330036, China

ARTICLE INFO

Keywords:
AOPs
Carbonate radical anion
Hydroxyl radical
Steady state concentrations
Transformation pathways

ABSTRACT

Reported herein is an investigation of the impact of water quality parameters on the formation of carbonate radical anion ($CO_3^{\bullet-}$) and hydroxyl radical ($HO^{\bullet}$) in UV/sodium percarbonate (UV/SPC) system versus in UV/hydrogen peroxide (UV/H_2O_2) system for bisphenol A (BPA) degradation in water. Pathways of $CO_3^{\bullet-}$ oxidation of BPA were proposed in this study based on the evolution of direct transformation products of BPA. Observed in this study, the degradation of BPA in the UV/SPC system was slower than that in the UV/H_2O_2 system in the secondary effluents collected from a local wastewater treatment plant due to the significant impact of coexisting constituents in the matrices on the former system. Single water quality parameter (*e.g.*, solution pH, common anion, or natural organic matter) affected radical formations and BPA degradation in the UV/SPC system in a way similar to that in the UV/H_2O_2 system. Namely, the rise of solution pH decreased the steady state concentration of $HO^{\bullet}$ resulting in a decrease in the observed pseudo first-order rate constant of BPA (k_{obs}). Chloride anion and sulfate anion played a negligible role over the examined concentrations; nitrate anion slightly suppressed the reaction at the concentration of 20 mM; bicarbonate anion decreased the steady state concentrations of both $CO_3^{\bullet-}$ and $HO^{\bullet}$ exerting significant inhibition on BPA degradation. Different extents of $HO^{\bullet}$ scavenging were observed for different types of natural organic matter in the order of fulvic acid > mixed NOM > humic acid. However, the impact was generally less pronounced on BPA degradation in the UV/SPC system than that in the UV/H_2O_2 system due to the existence of $CO_3^{\bullet-}$. The results of this study provide new insights into the mechanism of $CO_3^{\bullet-}$ based oxidation and new scientific information regarding the impact of water quality parameters on BPA degradation in the sytems of UV/SPC and UV/H_2O_2 from the aspect of reactive radical formation, which have reference value for UV/SPC application in wastewater treatment.

1. Introduction

Bisphenol A (BPA) is an essential compound for synthesizing epoxy resins and polycarbonate plastics that are widely used in the manufacture of many products, such as plastic bottles, food can linings, and food/beverage storage containers (Staples et al., 1998). From 1993 to 2007, the weight of BPA released into the environment increased nearly 5 times from 109 tons (Staples et al., 1998) to 500 tons (USEPA, 2010). Such extensive use of BPA has caused great concern on its potential damage to environmental sustainability. The occurrence of BPA in a variety of media, such as water, air, and soil, has been reported (Fan et al., 2021, Parto et al., 2021, Vandenberg et al., 2007). Evidence has shown that exposure to BPA at environmental concentrations is detrimental to wildlife over time (Crain et al., 2007, Sharma and Chadha, 2021). Epidemiological studies have indicated that BPA exposure can induce adverse health consequences including cancer, endocrine disorder, metabolic disturbance, and neurodevelopment problems (Gao et al., 2021, Goralczyk, 2021, Mercogliano et al., 2021, Senra and Lúcia

* Corresponding authors.
E-mail addresses: duanxdi@gmail.com (X. Duan), dionysdd@ucmail.uc.edu (D.D. Dionysiou).

https://doi.org/10.1016/j.watres.2022.118457
Received 7 November 2021; Received in revised form 9 April 2022; Accepted 12 April 2022
Available online 20 April 2022

Fonseca, 2021). For these reasons, finding efficient technologies for BPA removal from wastewater is essential for effective protention of environmental and public safety.

UV/hydrogen peroxide (UV/H_2O_2) system has been extensively studied and applied for wastewater treatment. In contrast, the knowledge of physical-chemical characteristics and environmental friendliness of UV/sodium percarbonate (UV/SPC) system remains scarce in the literature. Our previous study (Gao et al., 2020) reported that BPA could be effectively degraded at pH 8.5 in Milli-Q water (resistivity ≤18.2 MΩ·cm at 25 °C) in the systems of UV/SPC and UV/H_2O_2 at similar degradation rates. Both hydroxyl radical ($HO^•$) and carbonate radical anion ($CO_3^{•-}$) were generated in the UV/SPC system for BPA degradation (Eqs. (1)–(5)). Although the second-order rate constant of $CO_3^{•-}$ towards BPA ($k_{CO_3^{•-}+BPA} = 2.23 \times 10^8$ M^{-1} s^{-1}) was smaller than that of $HO^•$ ($k_{HO^•+BPA} = 1.02 \times 10^{10}$ M^{-1} s^{-1} (Rosenfeldt and Linden, 2004)), the steady state concentration of $CO_3^{•-}$ ($[CO_3^{•-}]_{ss} = 2.3 \times 10^{-12}$ M) was significantly higher than that observed for $HO^•$ ($[HO^•]_{ss} = 1.82 \times 10^{-14}$ M). In the same work, four pathways of BPA degradation in the UV/SPC system were proposed based on the identified transformation products (TPs).

The above-mentioned work (Gao et al., 2020) generates interest on the role of $CO_3^{•-}$ in BPA transformation in UV/SPC system. However, that work neither differentiated the specific pathways of BPA transformation by $CO_3^{•-}$ from the comprehensive oxidation in UV/SPC system, nor investigated the impact of water quality parameters (*e.g.*, solution pH, common anions, and natural organic matter (NOM)) on BPA degradation in UV/SPC system. In this study, the particular mechanism of BPA transformation by $CO_3^{•-}$ was investigated by tracking the evolution of direct TPs of BPA transformed by $CO_3^{•-}$. The impact of solution pH (3.0, 8.5, and 10.7), common anions (Cl^-, SO_4^{2-}, NO_3^- and HCO_3^-), and NOM (fulvic acid (FA), humic acid (HA), and mixed (NOM)) on the formation of both reactive radicals and the BPA degradation in the systems of UV/SPC and UV/H_2O_2 was investigated because common water quality parameters may interfere in the formation of $CO_3^{•-}$ and $HO^•$ through Eq. (1) - (17) listed in Table 1. Moreover, BPA degradation in the secondary effluents before chlorination from a regional wastewater treatment plant (WWTP) was performed to evaluate the real impact of water qualities on BPA degradation in the UV/SPC system. The overall objective of this study is to contribute a better understanding of the reaction mechanism of BPA transformation by $CO_3^{•-}$, to enrich the body of knowledge for UV/SPC system, and to provide insights into the potential of UV/SPC sysem as an alternative to UV/H_2O_2 system in specific scenarios and cases for wastewater treatment.

Table 1
Reactions and related parameters involved in this study.

Eq. No.	Reaction	Reaction constant (M^{-1} s^{-1})	Reference
(1)	$H_2O_2 \Leftrightarrow^{h\nu} 2HO^•$	$\Phi = 1$	(Baxendale and Wilson 1957)
(2)	$HO^• + HCO_3^- \rightarrow CO_3^{•-} + H_2O$	$k = 8.5 \times 10^6$	(Buxton et al. 1988)
(3)	$HO^• + CO_3^{2-} \rightarrow CO_3^{•-} + HO^-$	$k = 3.9 \times 10^8$	(Buxton et al. 1988)
(4)	$HO^• + BPA \rightarrow Products$	$k = 1.0 \times 10^{10}$	(Rosenfeldt and Linden 2004)
(5)	$CO_3^{•-} + BPA \rightarrow Products$	$k = 2.2 \times 10^8$	(Gao et al. 2020)
(6)	$HO^• + HO^- \rightarrow O^{•-} + H_2O$	$k = 1.2 \times 10^{10}$	(Buxton et al. 1988)
(7)	$CO_3^{•-} + CO_3^{•-} \rightarrow CO_2 + CO_4^{2-}$	$k = 6.2 \times 10^6$	(Neta et al. 1988)
(8)	$Cl^- + HO^• \rightarrow ClOH^{•-}$	$k = 4.3 \times 10^9$	(Jayson et al. 1973)
(9)	$ClOH^{•-} \rightarrow Cl^- + HO^•$	$k = 6.1 \times 10^9$	(Jayson et al. 1973)
(10)	$ClOH^{•-} + H^+ \rightarrow Cl^• + H_2O$	$k = 2.1 \times 10^{10}$	(Jayson et al. 1973)
(11)	$Cl^• + Cl^- \rightarrow Cl_2^{•-}$	$k = 2.1 \times 10^{10}$	(Jayson et al. 1973)
(12)	$NO_3^- \xrightarrow{h\nu} ONOO^-$	$\Phi = 0.102 \pm 0.002$	(Goldstein and Rabani 2007)
(13)	$ONOO^- + HO^• \rightarrow NO^• + O_2 + HO^-$	$k = 4.8 \times 10^9$	(Goldstein et al. 1998)
(14)	$NO_3^- \xrightarrow{h\nu} NO_2^• + O^{•-}$	$\Phi = 0.037 \pm 0.004$	(Goldstein and Rabani 2007)
(15)	$^1NOM \xrightarrow{h\nu} {}^3NOM^*$		(Turro et al. 2009)
(16)	$^3NOM^* + {}^3O_2 \rightarrow {}^1O_2 + {}^1NOM$		(Parker et al. 2013)
(17)	$^3NOM^* + H_2O \rightarrow HO^• + {}^1NOM$		(Dong and Rosario-Ortiz 2012)

2. Material and methods

2.1. Material

The main chemicals used in this study were H_2O_2 (50% w/w, Fisher Scientific, Pittsburgh, PA, USA), SPC (available as H_2O_2 20-30% w/w aqueous solution, Sigma Aldrich, St. Louis, MO, USA), and BPA (≥99% Sigma Aldrich, St. Louis, MO, USA). The molar ratio of Na_2CO_3 to H_2O_2 in the commercially purchased SPC in this study was experimentally determined and corresponded to 1: 1.15. Information about other chemicals, please see **Text S1** provided in **Supplementary Material (SM)**. Solution pH was adjusted with H_2SO_4 and maintained with sodium carbonate itself dissociated from SPC or phosphate buffer. The measured values of examined water quality parameters before and after corresponding experiments of single parameter impact are presented in Table 2. The field water samples used in this study were secondary effluents before chlorination collected from a regional WWTP in March (WE Mar.), June (WE Jun.), September (WE Sep.), and December (WE Dec.), and directly applied without any further processing. Related water qualities of these samples are summarized in Table 3.

2.2. Photochemical degradation and analytical methods

Since the literature does not report any information regarding the UV spectrum for SPC activation, we performed a scan of light absorbance for SPC over 200 - 400 nm (UV wavelength range in the non-vacuum environment). The obtained spectrum (Fig. S1) shows that UV with wavelength shorter than 300 nm is good for SPC activation. However, too short wavelength requires too high energy input, and the UV light used in most applied technologies is emitted from low-pressure lamps at a wavelength of 253.7 nm (USEPA, 1999). Thus, UV 253.7 was chosen in this study to activate SPC for UV/SPC system in consideration of compatibility to existing water and wastewater treatment processes and energy efficiency.

The degradation experiments, either for BPA removal or TP analysis

Table 2
Measured values of examined water qualtiy parameters (before/after experiments) in the study of single parameter impact on BPA degradation in UV/SPC and UV/H_2O_2 systems.

Object Parameter	Measured Value		
Solution pH	**pH Meter Reading**		
	3	**8.5**	**10.7**
pH	3.00/3.03	8.55/8.58	10.71/10.68
Common Anion	**Concentration (mM)**		
	5 mM	**10** mM	**20** mM
Cl^-	5.05/5.01	9.93/9.89	19.83/19.85
SO_4^{2-}	5.03/4.93	9.99/10.01	20.03/20.32
NO_3^-	5.13/5.10	9.95/9.91	19.63/19.71
HCO_3^-	5.08/4.93	9.95/9.71	19.50/19.16
NOM	**Concentration (mg L^{-1} TOC)**		
	5 mg L^{-1} **TOC**	**10** mg L^{-1} **TOC**	**20** mg L^{-1} **TOC**
Humic Acid	5.70/5.63	10.47/10.81	19.77/20.77
Mixed NOM	5.67/5.68	10.32/10.28	19.88/19.93
Fulvic Acid	5.59/5.99	11.19/11.98	20.95/20.45
	Absorbance @ 253.7 nm		
	5 mg L^{-1} **TOC**	**10** mg L^{-1} **TOC**	**20** mg L^{-1} **TOC**
Humic Acid	0.25/0.24	0.46/0.45	0.94/0.93
Mixed NOM	0.16/0.16	0.44/0.45	0.82/0.83
Fulvic Acid	0.13/0.14	0.34/0.32	0.75/0.77

Table 3
Water qualities of collected secondary effluents.

Sample	Original pH	Absorbance@ 254 nm	TOC(mg L^{-1})	Cl^- (mg L^{-1})	SO_4^{2-} (mg L^{-1})	NO_3^- (mg L^{-1})	Alkalinity(mg L^{-1} $CaCO_3$)
WE Mar.	7.49	0.1478	7.87	131	70	6	45
WE Jun.	7.28	0.3265	17.40	299	70	3	49
WE Sep.	7.67	0.1751	6.78	222	50	3	52
WE Dec.	7.69	0.1732	5.17	157	60	4	50

purpose, were adapted from those described in our previously published paper (Gao et al., 2020). Please refer to **Text S2** in **SM** for more details.

The methods used for the measurement of BPA concentration and the identification of TPs were similar to those reported in the same paper as degradation experiments (Gao et al., 2020). The methods for determination of water quality parameters were described in detail in **SM**. The statistical analysis was adapted from published manual (Lai et al., 2022). For more information, please see **Text S3** in **SM**.

2.3. Calculations

The reactions performed in this study were assumed to be pseudo first-order. The rate of pseudo first-order reaction (r) can be expressed as Eq. (18) where F is UV fluence (*i.e.*, UV flux × time, mJ cm^{-2}), $[BPA]_{(F)}$ is the concentration of BPA (mM) at the fluence of F, and k_{obs} is the observed pseudo first-order rate constant (cm^2 mJ^{-1}). Integration of r (Eq. (19)) finds linear relationship between $\ln\frac{[BPA]_{(F)}}{[BPA]_0}$ and F (Eq. (20)). By plotting $\ln\frac{[BPA]_{(F)}}{[BPA]_0}$ against F, k_{obs} can be determined and is the negative value of the slope.

$$r = -\frac{d[BPA]_{(F)}}{dF} = k_{obs}[BPA]_{(F)} \tag{18}$$

$$\int_0^F -\frac{d[BPA]_{(F)}}{[BPA]_{(F)}} = -k_{obs}\int_0^F dF \tag{19}$$

$$\ln\frac{[BPA]_{(F)}}{[BPA]_0} = -k_{obs}F \tag{20}$$

Because the curves plotted from the data obtained (too many figures to provide) met the linear requirement, the assumption was valid and the k_{obs} were determined accordingly. Steady state concentrations of $HO^\bullet$ and $CO_3^{\bullet-}$ were assumed in this study since the concentrations of H_2O_2 and carbonate species did not change significantly before and after experiments. The BPA degradation using only direct UV photolysis or only the oxidant was found to be negligible. The results of BPA degradation in these two conditions were presented in **SM** of our previous paper (Gao et al., 2020). The calculation of $[HO^\bullet]_{ss}$ and $[CO_3^{\bullet-}]_{ss}$ was described in detail in the same paper (Gao et al., 2020). Briefly, the competitive degradation of BPA and PhOH in the UV/SPC system is expressed by Eqs. (21,22), where $k_{obs,UV+SPC+BPA}$ is the observed pseudo first-order rate constant of BPA (cm^2 mJ^{-1}) in competition with PhOH in the UV/SPC system, $k_{obs,\ UV+SPC+PhOH}$ is the observed pseudo first-order rate constant of PhOH (cm^2 mJ^{-1}) in competition with BPA in the UV/SPC system, $[\overline{UV}] = 0.093$ mW cm^{-2}, $k_{HO^\bullet+\ BPA} = 1.02\times10^{10}$ M^{-1} s^{-1}, $k_{CO_3^{\bullet-}+BPA} = 2.28\times10^8$ M^{-1} s^{-1}, $k_{HO^\bullet+PhOH} = 1.4\times10^{10}$ M^{-1} s^{-1}, and $k_{CO_3^{\bullet-}+PhOH} = 1.2\times10^8$ M^{-1} s^{-1}. By solving this set of equations, the $[HO^\bullet]_{ss}$ and $[CO_3^{\bullet-}]_{ss}$ were determined.

$$k_{obs,UV+SPC+BPA}[\overline{UV}] = k_{HO^\bullet+\ BPA}[HO^\bullet]_{ss} + k_{CO_3^{\bullet-}+BPA}[CO_3^{\bullet-}]_{ss} \tag{21}$$

$$k_{obs,\ UV+SPC+PhOH}[\overline{UV}] = k_{HO^\bullet+PhOH}[HO^\bullet]_{ss} + k_{CO_3^{\bullet-}+PhOH}[CO_3^{\bullet-}]_{ss} \tag{22}$$

The degradation of BPA in the UV/H_2O_2 system was expressed by Eq. (23), where $k_{obs,\ UV+H_2O_2+BPA}$ is the observed pseudo first-order rate constant of BPA (cm^2 mJ^{-1}) in the UV/H_2O_2 system. The $[HO^\bullet]_{ss}$ in the UV/H_2O_2 system was quantified by substituting in the $k_{obs,UV+H_2O_2+BPA}$ obtained from experiments.

$$k_{obs,UV+H_2O_2+BPA}[\overline{UV}] = k_{HO^\bullet+\ BPA}[HO^\bullet]_{ss} \tag{23}$$

The removal of BPA by $CO_3^{\bullet-}$ ($R_{CO_3^{\bullet-}}$) and by $HO^\bullet$ ($R_{HO^\bullet}$) and the contribution of $CO_3^{\bullet-}$ to total BPA degradation ($R_{CO_3^{\bullet-}}/R_{total}$) were calculated with a method reported in the literature (Huang et al., 2018). Summarizing, the $R_{CO_3^{\bullet-}}$ and $R_{HO^\bullet}$ were determined through Eq. (24) and Eq. (25), respectively, where t is the reaction time (s), $[BPA]_0$ is the initial concentration of BPA (mM), and $[BPA]_{(t)}$ is the concentration of BPA (mM) at time t. The total removal of BPA in the UV/SPC system (R_{total}) was calculated through Eq. (26) where R_{others} is the removal of BPA by minor radicals which was proven to be negligible in our previous paper (Gao et al., 2020). Therefore, $R_{CO_3^{\bullet-}}/R_{\text{total}}$ was quantified using Eq. (27).

$$R_{CO_3^{\bullet-}} = \frac{\int_0^t k_{CO_3^{\bullet-}+BPA}[CO_3^{\bullet-}]_{ss}[BPA]_{(t)}dt}{[BPA]_0} = k_{CO_3^{\bullet-}+BPA}[CO_3^{\bullet-}]_{ss}\int_0^t\frac{[BPA]_{(t)}}{[BPA]_0}dt \tag{24}$$

$$R_{HO^\bullet} = \frac{\int_0^t k_{HO^\bullet+BPA}[HO^\bullet]_{ss}[BPA]_{(t)}dt}{[BPA]_0} = k_{CO_3^{\bullet-}+BPA}[HO^\bullet]_{ss}\int_0^t\frac{[BPA]_{(t)}}{[BPA]_0}dt \tag{25}$$

$$R_{total} = R_{CO_3^{\bullet-}} + R_{HO^\bullet} + R_{others} = 1 - \frac{[BPA]_{(t)}}{[BPA]_0} \approx R_{CO_3^{\bullet-}} + R_{HO^\bullet} \tag{26}$$

$$R_{CO_3^{\bullet-}} \Big/ R_{total}(\%) = \frac{R_{CO_3^{\bullet-}}}{R_{total}}\ 100\% \tag{27}$$

3. Results and discussion

3.1. BPA transformation by carbonate radical anion

In order to reveal the mechanism of BPA transformation by $CO_3^{\bullet-}$, BPA degradation tests were conducted in direct UV photolysis control and in UV/SPC/t-BuOH system. Because BPA degradation in the direct UV photolysis control is almost negligible as observed in our previous work (Gao et al., 2020), and excess t-BuOH ($k_{HO^\bullet+\ t-BuOH}\times[t-BuOH] \gg k_{HO^\bullet+\ BPA}\times[BPA]$) can quench BPA reaction with $HO^\bullet$, BPA transformation in the UV/SPC/t-BuOH system is primarily attributed to $CO_3^{\bullet-}$ oxidation. The TPs found for each system and their evolution profiles with UV fluence are shown in Tables S2–S4.

Under direct UV photolysis, BPA degradation was extremely slow and insignificant. Yet, we still managed to detect the hydroxylated TPs (A1 & A3), quinone TPs (A2 & A3) and single ring TP (C1) in this system, suggesting that direct UV photolysis of BPA occurs mainly through hydroxylation of phenolic ring, quinonation of phenolic ring, and cleavage of the linking bond between phenolic ring and isopropylidene group. Moreover, all TPs appeared from the beginning and continuously accumulated over the entire test range of UV fluence (Table S3), which means BPA is being continuously transformed into these TPs. This result confirms that UV photolysis of BPA is slow, and therefore, may be not able to achieve complete oxidation.

In the UV/SPC/t-BuOH system, the hydroxylated TPs, quinone TPs, and single-ring TPs were also detected, and the relative abundance of

these TPs was much higher than that observed in the direct UV photolysis. This implies that the phenolic ring and the linking bond between phenolic ring and isopropylidene group are common reactive sites for direct UV photolysis and $CO_3^{\bullet-}$ oxidation of BPA. In addition, isopropylidene-modified TPs were only detected in the UV/SPC/t-BuOH system which suggests that $CO_3^{\bullet-}$ attack can activate the isopropylidene group facilitating BPA degradation. As for carboxylic TPs, they were uniquely detected in the UV/SPC/t-BuOH system, indicating that $CO_3^{\bullet-}$ oxidation of BPA realizes the cleavage of benzene ring, and therefore, is a more complete oxidation process than direct UV photolysis.

The evolution of TPs with UV fluence in the UV/SPC/t-BuOH system (Table S4) shows that single-hydroxylated TPs were formed at UV fluence between 0–1009 mJ cm^{-2}. Above 1009 mJ cm^{-2}, multi-hydroxylated TPs started to form, and were extensively detected at high UV fluence. This demonstrates that multi hydroxylation of BPA is relatively difficult and slower than single hydroxylation. It is worth mentioning that hydroxylated TPs of B1 & B2, C1 & C2, and C5 & C6 were consecutively evolved consecutivelyindicating that ring hydroxylation of isopropylidene-modified TPs and single-ring TPs occurs after isopropylidene modification and cleavage of linking bond between phenolic ring and isopropylidene group. In addition, the massive production of carboxylic TPs at higher UV fluences confirms that ring cleavage is the result of continuous oxidation.

Based on the discussion above, the pathways of BPA degradation by $CO_3^{\bullet-}$ was proposed as depicted in Fig. 1: **(A) Hydroxylation:** the interaction of $CO_3^{\bullet-}$ with the electron rich phenolic ring causes instability in the electron configuration of aromatic ring. One electron is transferred from the phenolic ring to $CO_3^{\bullet-}$ generating a BPA radical cation. The addition of a hydroxyl group to the BPA radical cation at the *ortho*-position of phenolic ring (Carbon No.2 or 4) in water containing molecular oxygen induces hydroxylation of BPA. The hydroxylation of BPA increases the density of electron on the phenolic ring, leading to multi hydroxylation of phenolic ring following the same mechanism. **(B) Oxidation Demethylation**: the attack of $CO_3^{\bullet-}$ to isopropylidene group abstracts a hydrogen atom and initiates a series of radical chain oxidation processes in the oxic environment, forming a demethylated BPA radical (d-BPA radical) and then isopropylidene modified TPs. The phenolic rings of isopropylidene-modified TPs are hydroxylated afterwards via the same mechanism as hydroxylation. **(C) Homolytic Cleavage**: the addition of hydroxyl group to BPA radical cation at the *para*-position of phenolic ring (Carbon No. 4) induces homolytic cleavage of the benzylic bond, forming hydroquinone and 4-isopropylphenol radicals. This also can be achieved by secondary β-scission as mentioned in our previous paper (Gao et al., 2020). Water solvent turns the 4-isopropylphenol radical into corresponding alcohols, ketones, and alkenes. Afterwards, hydroxylation of the phenolic rings of generated TPs is carried out . Ultimately, continuous oxidation of TPs generates carboxylic TPs and small molecular acids step by step until complete mineralization of BPA.

As opposed to the general pathways of BPA degradation in UV/SPC system proposed in our previous paper (Gao et al., 2020) which are a combined result of $HO^{\bullet}$ and $CO_3^{\bullet-}$ oxidation, the reaction pathways proposed here are specific to BPA transformation by $CO_3^{\bullet-}$, a step further from our previous work. The discussion in this section confirms the initiation of phenolic ring oxidation by $CO_3^{\bullet-}$ through one electron transfer, proposes a new mechanism for isopropylidene modification through oxidation demethylation by $CO_3^{\bullet-}$ and a new mechanism for isopropylidene bridge cleavage via homolytic cleavage according to the chemical properties of $CO_3^{\bullet-}$, and finds that $CO_3^{\bullet-}$ attack can activate the isopropylidene group to facilitate BPA degradation.

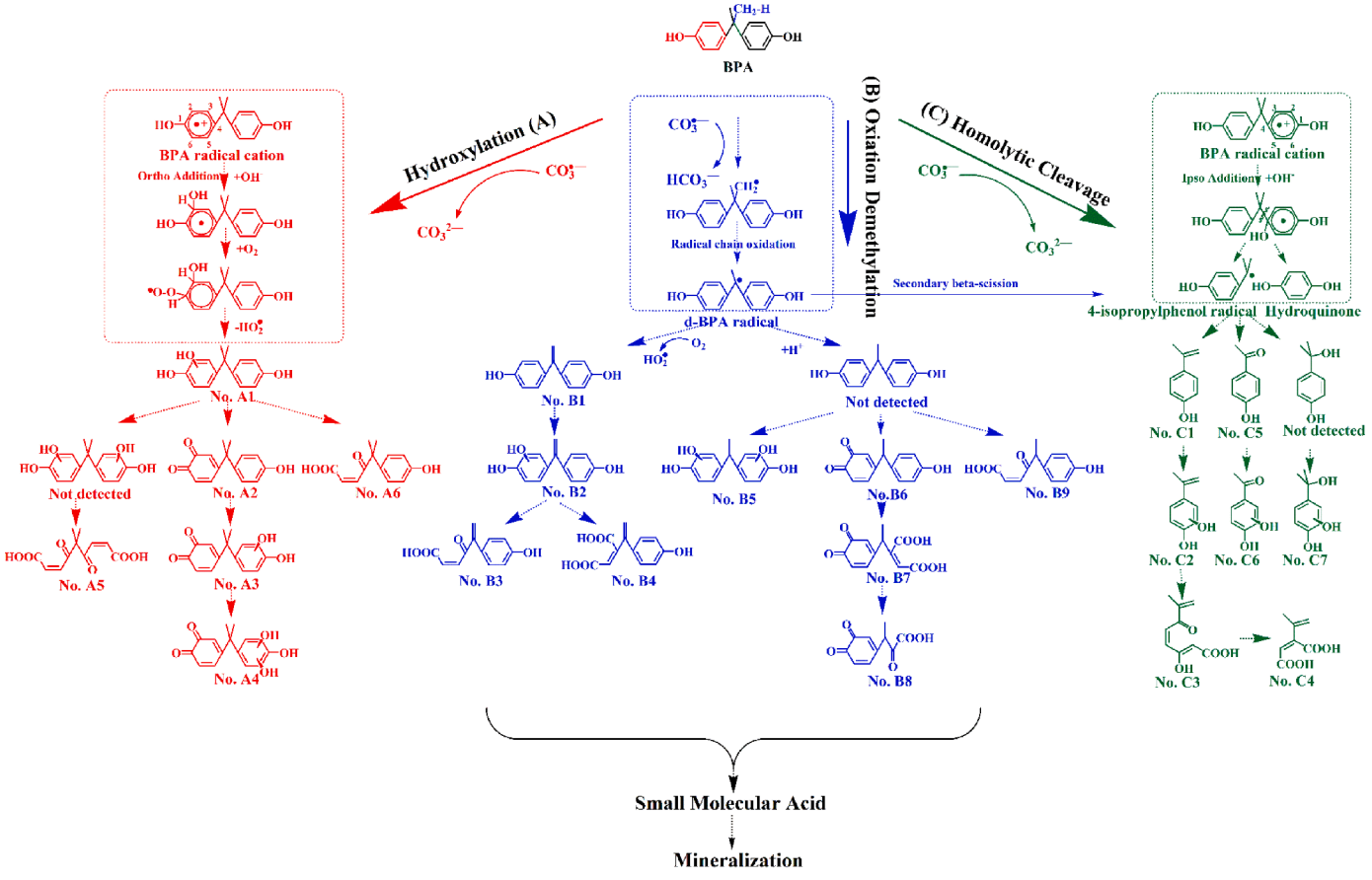

Fig. 1. Proposed reaction pathways of BPA transformation by $CO_3^{\bullet-}$.

3.2. BPA degradation in the secondary effluents

To evaluate the general impact of water qualities on the treatment performance of UV/SPC process, BPA degradation was conducted in the secondary effluents from a regional WWTP collected in different months. These water samples are different from the ones reported in our previous work regarding collection time and water qualities (refer to Section 2.1 for more information about these samples). The results of BPA degradation by UV/SPC process were compared with those by UV/H_2O_2. As shown in Fig. 2, BPA degradation byUV/SPC process was not as efficient as that by UV/H_2O_2 process in the secondary effluents without pH change and at neutral/alkaline pH. The acidification of matrix significantly increased the observed pseudo first-order rate constant of BPA degradation by UV/SPC process ($k_{obs,UV/SPC}$) to the level equal to or higher than the observed pseudo first-order rate constant of BPA degradation by UV/H_2O_2 process ($k_{obs,UV/H_2O_2}$). The efficiencies of BPA degradation by UV/SPC and UV/H_2O_2 processes were reported to be comparable in Milli-Q water (Gao et al., 2020), so the obviously smaller $k_{obs,UV/SPC}$ than $k_{obs,UV/H_2O_2}$ in the secondary effluents underlines the stronger interference of water qualities on BPA degradation by UV/SPC process than on BPA degradation by UV/H_2O_2.

Multi-parameter variation partitioning and hierarchical partitioning for the data obtained from the above experiments were performed to evaluate the individual contributions of measured water quality parameters of collected secondary effluents to the total impact of water qualities on BPA degradation in the UV/SPC system in these matrices. The obtained contribution percentages are displayed in Fig. 2b which shows the independent contributions of pH, TOC, and alkalinity to the total impact of secondary effluent qualities are 59.39%, 34.63%, and 10.22%, respectively. This means pH, TOC and alkalinity are three major water quality parameters that impact BPA degradation in the UV/SPC system in secondary effluents. This result is consistent with the observations in the impact of single water quality parameter on BPA degradation as discussed in the following sections where the change of pH, TOC, and HCO_3^- significantly altered the efficiency of BPA degradation in UV/SPC system.

In the following sections, BPA degradation in the systems of UV/SPC and UV/H_2O_2 with different pH, common anions, and NOM were investigated to shed light on the understanding of how these water quality parameters affect BPA degradation and how they interfere in the formation of $HO^\bullet$ and $CO_3^{\bullet-}$ in these systems.

3.3. Impact of solution pH

To study the impact of solution pH on BPA degradation and the formation of reactive radicals in the systems of UV/SPC and UV/H_2O_2, Milli-Q water was used as reaction solution to exclude interferences from other water quality parameters. Solution pH of 3.0, 8.5, and 10.7 were chosen to mimic the pH conditions of concentrated landfill leachate (pH = 3), finished sewage (pH = 8.5), and water dissolving of 1 M SPC (pH = 10.7).

The increase of pH decreased k_{obs} in both systems (Fig. 3a). One possible cause can be the decrease of $[HO^\bullet]_{ss}$ for the following two reasons. First, the concentration of HO^- ($[HO^-]$) increases with the increase of pH. For example, the $[HO^-]$ at pH 3.0 is only about 10^{-5} μM while the $[HO^-]$ at pH 10.7 increases to over 500 μM. Because the quantum yield of $HO^\bullet$ produced in UV photolysis of H_2O_2 remains constant at different pH (Khan et al., 2014), the scavenging of $HO^\bullet$ by HO^- (Eq. (6)) decreases $[HO^\bullet]_{ss}$ in the alkaline environment. Second, the phenolic ring of BPA is gradually deprotonated into phenolate anion with the increase of pH (Clara et al., 2004, Westall et al., 1985). The phenolate anion has strong UV absorbance (Gillam and Stern, 1954) thus competing against H_2O_2 for UV radiation photons resulting in the decrease of $HO^\bullet$ generation. The determined steady state concentrations of reactive radicals ($[radical]_{ss}$) (Fig. 3b) at different pH confirms the decrease of $[HO^\bullet]_{ss}$ in both systems. When the solution pH was increased from 3.0 to 10.7, the $[HO^\bullet]_{ss}$ in the UV/H_2O_2 system decreased from 1.0 × 10^{-12} M to 2.3 × 10^{-13} M; the $[HO^\bullet]_{ss}$ in the UV/SPC system decreased from 3.9 × 10^{-14} M to 3.3 × 10^{-16} M. In UV/SPC system, the speciation of BPA at high pH values can be another cause of decreased value of k_{obs}. According to reported data in literature (Clara et al., 2004, Staples et al., 1998), the pKa value of BPA falls between 9.6–11.3, which means BPA is more likely to be electronegative at pH > 9.6. Because $CO_3^{\bullet-}$ is negatively charged as well, the electrostatic repulsion between $CO_3^{\bullet-}$ and BPA decreases the reactivity of $CO_3^{\bullet-}$ towards BPA resulting in the decreased efficiency of BPA degradation in the akaline conditions.

Moreover, the $[CO_3^{\bullet-}]_{ss}$ remained around 1.8 × 10^{-12} M in the examined pH range of 3.0 - 10.7 (Fig. 3b), demonstrating the negligible impact of solution pH on $CO_3^{\bullet-}$ formation. The increase of solution pH from 3.0 to 10.7 increased $R_{CO_3^{\bullet-}}$ from 39% to 79%, indicating that BPA oxidation by $CO_3^{\bullet-}$ increases with the increase of solution pH. The $R_{CO_3^{\bullet-}}/R_{total}$ increased from 43% at pH 3.0 to 99% at pH 10.7, illustrating that $CO_3^{\bullet-}$ gradually becomes the key species responsible for BPA degradation as the solution pH increases. Because the pH impact on BPA

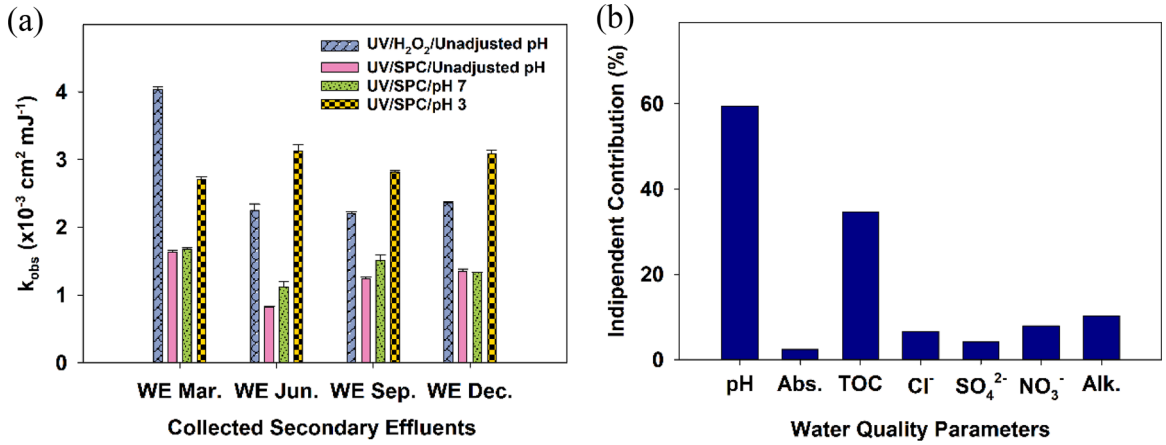

Fig. 2. (a) The observed pseudo first-order rate constants of BPA degradation (k_{obs}) in the secondary effluents before chlorination from a wastewater treatment plant, collected in March (WE Mar.), June (WE Jun.), September (WE Sep.), and December (WE Dec.); (b) The independent contribution of each water quality parameter to the total impact of water qualities on BPA degradation by UV/SPC in the secondary effluents. Unadjusted pH means no pH adjustment after the addition of oxidants. The pH of the UV/H_2O_2 system with unadjusted pH was maintained around 7 by 5 mM phosphate buffer. The pH of the UV/SPC system with unadjusted pH was maintained around 9.0 by the system itself due to the alkalinity and the buffering capacity of Na_2CO_3 in SPC. $[H_2O_2]_0$ = 1.15 mM, $[SPC]_0$ =1 mM, $[BPA]_0$ = 2 μM, [UV] = 0.1 mW cm^{-2}.

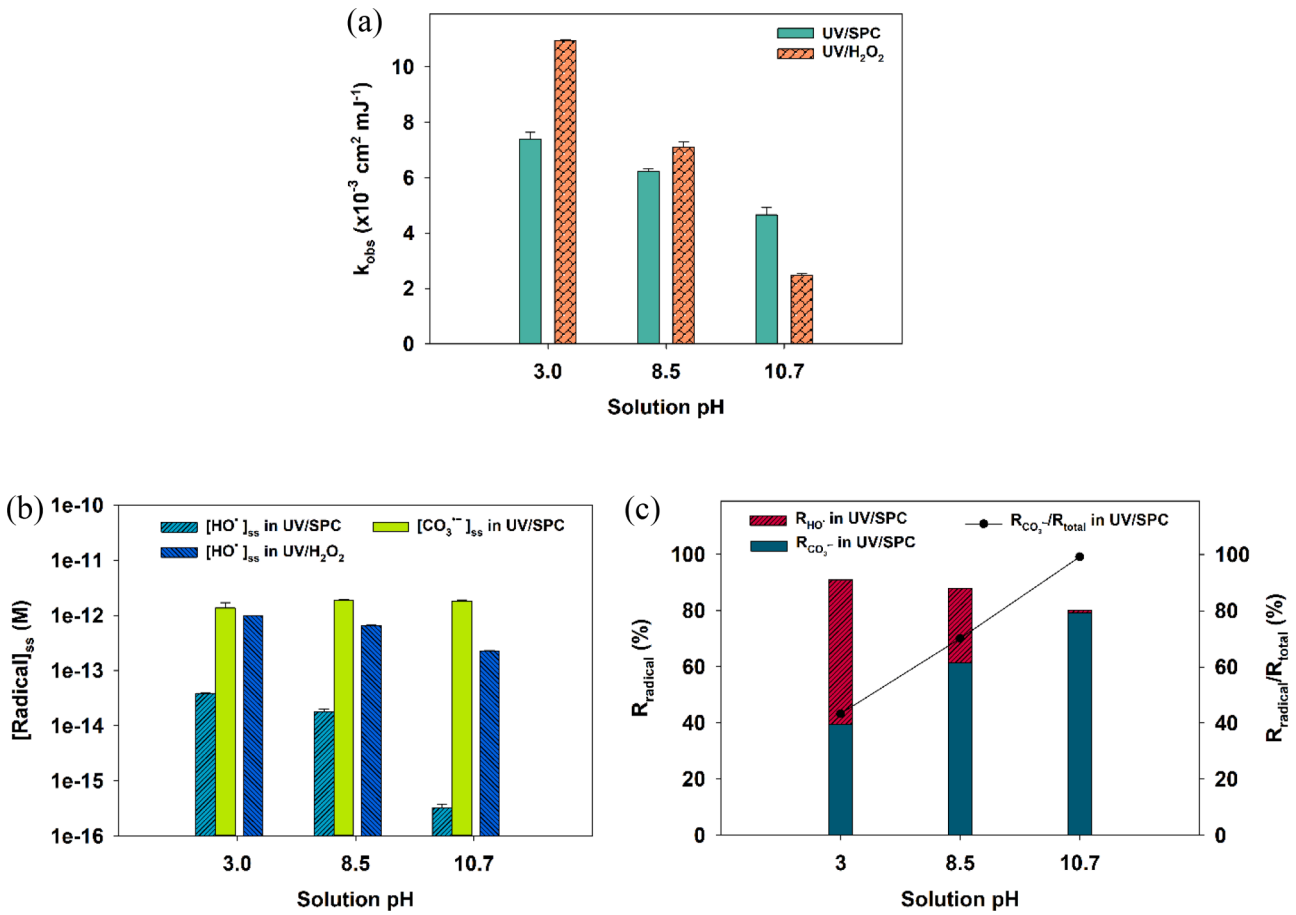

Fig. 3. (a) The observed pseudo first-order rate constant of BPA degradation (k_{obs}) at different pH values; (b) The steady state concentrations of reactive radicals ([radical]$_{ss}$) at different pH values; (c) The removal of BPA by reactive radicals ($R_{radical}$, displayed in bar) and the contribution of $CO_3^{\bullet-}$ to BPA degradation ($R_{CO_3^{\bullet-}}/R_{total}$, displayed in line) at different pH values. $[H_2O_2]_0$ = 1.15 mM, $[SPC]_0$ =1 mM, $[BPA]_0$ = 2 μM, [UV] = 0.1 mW cm^{-2}.

degradation in the UV/SPC system is mitigated by such responses of $CO_3^{\bullet-}$, $k_{obs,UV/SPC}$ decreased more slowly than $k_{obs,UV/H_2O_2}$ with the increase of solution pH.

3.4. Impact of common anions

Anions that are ubiquitous in natural aquatic environment may pose beneficial or adverse effects on the performance of different AOPs (Parsons, 2004). Four common anions in water (*i.e.*, Cl^-, SO_4^{2-}, NO_3^-, and HCO_3^-) were chosen in this study to investigate the impact of common anions at four common concentrations (0, 5, 10, and 20 mM). At pH 8.5, the dominant species of carbonic system is HCO_3^-, thus the impact of HCO_3^- instead of the impact of CO_3^{2-} was investigated in this study. As shown in Fig. 4a-d, the impact of the chosen anions on BPA degradation in the UV/SPC system were similar to that observed in the UV/H_2O_2 system. Specifically, Cl^- and SO_4^{2-} had negligible impact, NO_3^- at concentration of 20 mM slightly inhibited BPA degradation, and HCO_3^- significantly decreased k_{obs} at all examined concentrations.

Possible reactions of Cl^- in both systems are shown in Eqs. (8)–(11). Neta et al. (1988) reported that Eq. (10,11) only take place under acidic condition and are negligible at pH 8.5. The formation and dissociation of $ClOH^{\bullet-}$ (Eqs. (8,9)) occurs at comparable rates, and Cl^- is nonreactive with $CO_3^{\bullet-}$. Therefore, Cl^- had little influence on BPA degradation.

The influence of SO_4^{2-} on BPA degradation was negligible in both systems. It is consistent with the fact that neither $HO^{\bullet}$ nor $CO_3^{\bullet-}$ appreciably reacts with SO_4^{2-}.

NO_3^-, a well-known photosensitizer, can initiate a series of reactions under light irradiation, producing reactive nitrogen species (RNS, *e.g.*, $ONOO^-$, O_2NOO^-, $NO_2^{\bullet}$, NO_2^-, $NO^{\bullet}$). Under the experimental condition in this study (*i.e.*, pH 8.5 and UV λ = 253.7 nm), the dominant reactions are expressed in Eqs. (12)–(14). Huang et al. (Huang et al., 2018) found that BPA could be degraded in UV/NO_3^- system ascribed to RNS oxidation, and the rate of BPA degradation in the UV/NO_3^- system was significantly enhanced in the presence of HCO_3^-. However, in this study, a slight inhibition was observed on the degradation of BPA in both systems with the addition of 20 mM NO_3^-. This is likely because: (1) the quantum yield of NO_3^- ($\Phi = 0.102 \pm 0.002$ Eq. (12) and $\Phi = 0.037 \pm 0.004$ Eq. (14)) is significantly lower than the quantum yield of H_2O_2 ($\Phi = 1$ Eq. (1)), thus RNS cannot be sufficiently generated in the UV systems containing H_2O_2; (2) at high concentration of 20 mM, the photosensitization of NO_3^- considerably decreases the incident photons for H_2O_2 activation and the generated RNS scavenges $HO^{\bullet}$ (Eq. (13)) in the system.

HCO_3^- displayed significant inhibition on the degradation of BPA in both systems and the inhibiting effect increased with the increasing concentration of HCO_3^- ($[HCO_3^-]$). Addition of HCO_3^- into UV/H_2O_2 system renders UV/H_2O_2 system the ability to generate $CO_3^{\bullet-}$ following the same reactions as those in UV/SPC system (Eqs. (1)–(3)). $HO^{\bullet}CO_3^{\bullet-}HCO_3^-HO^{\bullet}HCO_3^-HCO_3^-$ $CO_3^{\bullet-}HCO_3^-$ $HCO_3^-]HCO_3^-CO_3^{\bullet-}HO^{\bullet}HCO_3^-]$ $HO^{\bullet}CO_3^{\bullet-}HCO_3^-R_{HO^{\bullet}}HCO_3^-$ $R_{CO_3^{\bullet-}}$ $HO^{\bullet}CO_3^{\bullet-}HCO_3^-HO^{\bullet}CO_3^{\bullet-}k_{obs}$ This is supported by the data displayed in Fig. 4e where the values of $[HO^{\bullet}]_{ss}$ and $[CO_3^{\bullet-}]_{ss}$ in the the UV/H_2O_2 system after addition of HCO_3^- were similar to those in the UV/SPC system. The plunge of $[HO^{\bullet}]_{ss}$ after the addition of HCO_3^- (Eq. (2)) is the reason for the sudden drop of k_{obs} in both systems. The gradual lower of $[CO_3^{\bullet-}]_{ss}$, as a result of the increased importance of Eq. (7) in HCO_3^- rich solutions, explains

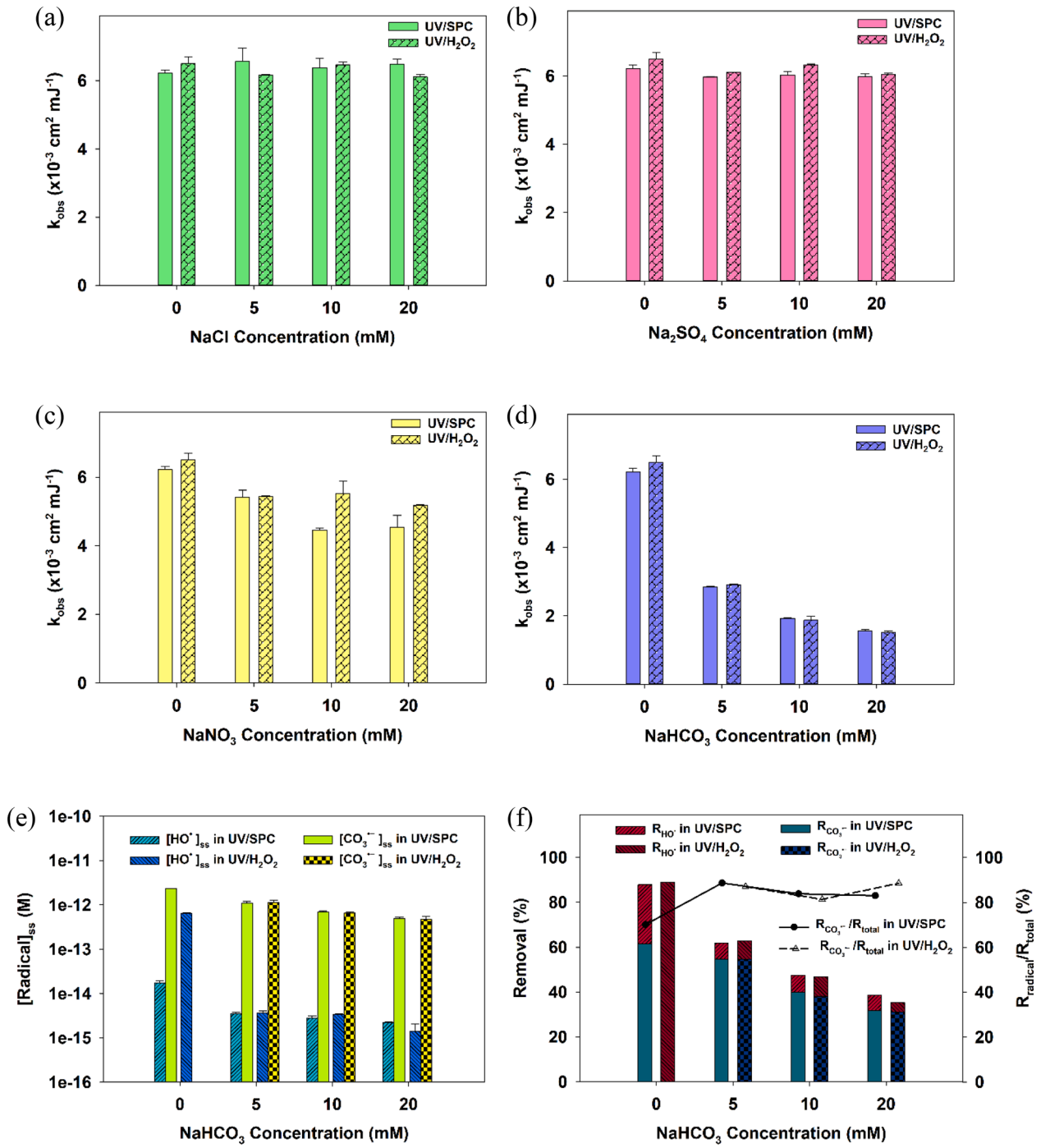

Fig. 4. The observed pseudo first-order rate constants of BPA degradation (k_{obs}) with the addition of different concentrations of (a) chloride anion, (b) sulfate anion, (c) nitrate anion, (d) bicarbonate anion; (e) The steady state concentrations of reactive species ($[radical]_{ss}$) at different concentrations of bicarbonate anion; (f) The removal of BPA by reactive radicals ($R_{radical}$, displayed in bar) and the contribution of $CO_3^{\bullet-}$ to BPA degradation ($R_{CO_3^{\bullet-}}/R_{total}$, displayed in line) at different concentrations of bicarbonate anion. $[H_2O_2]_0$ = 1.15 mM, $[SPC]_0$ =1 mM, $[BPA]_0$ = 2 μM, [UV] = 0.1 mW cm^{-2}, pH 8.5.

why the k_{obs} gradually decreases with the increase of $[HCO_3^-]$. In the meanwhile, the $R_{HO\bullet}$ and $R_{CO_3^{\bullet-}}$ decreased proportionally to k_{obs} and the $R_{CO_3^{\bullet-}}/R_{total}$ kept nearly constant regardless of $[HCO_3^-]$ change (Fig. 4f).

In addition, the $R_{CO_3^{\bullet-}}/R_{total}$ in the UV/H_2O_2 system remained between 81% and 88% after the addition of HCO_3^- (scatter line with empty triangle in Fig. 4f); the $R_{CO_3^{\bullet-}}/R_{total}$ in the UV/SPC system was kept between 83% and 89%, although the addition of 5 mM HCO_3^- increased $R_{CO_3^{\bullet-}}/R_{total}$ from 70% to 88% due to the sharp decrease of $[HO^\bullet]_{ss}$ (scatter line with solid circle in Fig. 4f). This points out that $CO_3^{\bullet-}$ is the main species responsible for BPA degradation in the presence of 5-20 mM HCO_3^- in both systems.

3.5. Impact of different types of natural organic matter

In addition to common anions, NOM is another category of substances present in natural waters that can significantly affect radical based AOPs (Autin et al., 2013, Fan et al., 2013, Li and Hu, 2018). In order to investigate the impact of NOM on the degradation of BPA in the systems of UV/SPC and UV/H_2O_2 , different types of NOM from

Suwannee River (FA, HA, and mixed NOM) were spiked into reaction solutions, at concentrations of 5, 10 and 20 mg L^{-1}.

The results displayed in Fig. 5a demonstrate that all types of NOM inhibited the degradation of BPA in both systems, with the inhibiting effects being increased as the concentration of NOM ([NOM]) was further increased. This could be because (1) NOM scavenges both reactive radicals of $HO^{\bullet}$ and $CO_3^{\bullet-}$; (2) NOM absorbs the incident light (absorbance @ 253.7 nm in Table 2) decreasing the light availability for the generation of $HO^{\bullet}$ and the subsequent generation of $CO_3^{\bullet-}$; (3) the formation of NOM-BPA complex decreases the accessibility of BPA by $CO_3^{\bullet-}$. As shown in Fig. 5b, the $[HO^{\bullet}]_{ss}$ in the UV/SPC system decreased from 1.77×10^{-14} M without NOM to 6.31×10^{-15} M, 4.47×10^{-15} M, and 2.18×10^{-15} M in the presence of 20 mg L^{-1} TOC of HA, mixed NOM, and FA, respectively; the $[CO_3^{\bullet-}]_{ss}$ in the UV/SPC system decreased from 1.9×10^{-12} M to 3.03×10^{-13} M, 5.12×10^{-13} M, and 4.80×10^{-13} M, respectively; the $[HO^{\bullet}]_{ss}$ in the UV/H_2O_2 system decreased from 6.50×10^{-13} M to 3.35×10^{-13} M, 1.96×10^{-13} M, and 1.85×10^{-13} M, respectively.

Different types of NOM inhibited BPA degradation in both systems following the sequence of FA > mixed NOM > HA. With the presence of different types of NOM at the concentration of 20 mM mg L^{-1} TOC, the $[CO_3^{\bullet-}]_{ss}$ in Fig. 5b stay close to each other in Fig. 5c are similar to each other; the decrease of $[HO^{\bullet}]_{ss}$ and $R_{HO^{\bullet}}$ follows the order of FA > mixed NOM > HA. Therefore, the different inhibiting effects of different types of NOMis related to the different effects of different types of NOM on the formation of $HO^{\bullet}$, which can be explained by light shadowing effect and photosensitivity. As presented in Table 2, the UV absorbance of different types of NOM is generally in the order of FA > mixed NOM > HA. The more light is absorbed by NOM, the less light is available for radical generation. Recent studies (Bodhipaksha et al., 2017; Loiselle et al., 2012; McCabe and Arnold, 2017; Schmitt et al., 2017) have shown that NOM can undergo photochemical reactions by which NOM with large molecular weight and active functional groups is excited from ground state (^{1}NOM) to excited state (^{3}NOM*) under UV or UV-Vis irradiation (Eq. (15)). ^{3}NOM* can transfer energy to dissolved oxygen or water generating reactive species such as $^1O_2$ and $HO^{\bullet}$ (Eq. (16)–(17)) which can promote the degradation of certain organics. In case of BPA, the oxidation of BPA by ^{3}NOM*-generated reactive species is supposed to be mainly achieved by $HO^{\bullet}$, because the redox potential of $^1O_2$ ($E_{^1O_2/O_2^{\bullet-}} =$ 0.65 V (Krumova and Cosa, 2016)) is much lower than that of $HO^{\bullet}$ ($E_{HO^{\bullet}/H_2O} = 2.33$ V (Krumova and Cosa, 2016)). Therefore, the inhibiting effect of NOM on BPA degradation can be mitigated by the photosensitive reactions as described above. As reported by Luo et al. (2018), FA mainly consists of small molecules (100 g $mole^{-1} \leq$ molecular weight $\leq$ 10,000 g $mole^{-1}$) and is a mixture of linear carbon chains and cyclic organic acids. These components determine that FA is less photosensitive and mainly exhibits scavenging effect. On the contrary, HA consists of large molecules (molecular weight $\geq$ 50,000 g $mole^{-1}$) and has aromatic or carbon rings containing oxygen, hydrogen, nitrogen or sulfur (Luo et al., 2018). Such composition of HA makes HA highly photosensitive resulting in the least decrease of $[HO^{\bullet}]_{ss}$. Because mixed NOM contains both FA and HA, the impact of mixed NOM is expected to fall

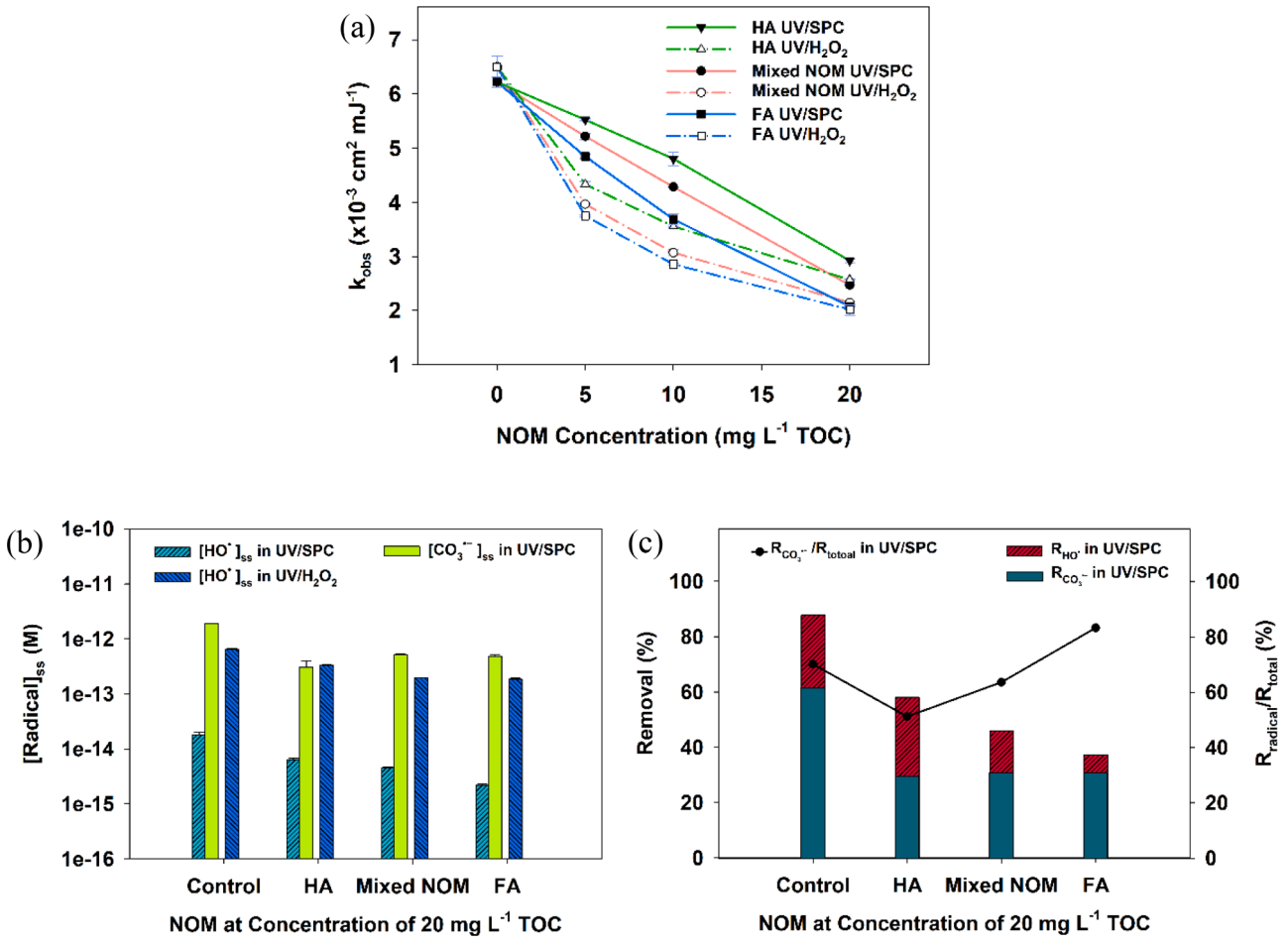

Fig. 5. (a) The observed pseudo first-order rate constants of BPA degradation (k_{obs}) in the presence of different concentrations of humic acid (HA), fulvic acid (FA), and mixed natural organic matter (Mixed NOM); (b) The steady state concentrations of reactive species ($[radical]_{ss}$) with the addition of different types of NOM at 20 mg L^{-1} TOC; (c) The removal of BPA by reactive radicals ($R_{radical}$, displayed in bar) and the contribution of $CO_3^{\bullet-}$ to BPA degradation ($R_{CO_3^{\bullet-}}/R_{total}$, displayed in line) with the addition of different types of NOM at 20 mg L^{-1} TOC. $[H_2O_2]_0 = 1.15$ mM, $[SPC]_0 = 1$ mM, $[BPA]_0 = 2$ μM, [UV] = 0.1 mW cm^{-2}, pH 8.5.

between HA and FA. Under this background, $CO_3^{\bullet-}$ oxidation of BPA contributes more to BPA degradation in the presence of FA than that in the presence of the other types of NOM. For example, as displayed in Fig. 5c, the $R_{CO_3^{\bullet-}}/R_{total}$ in the presence of FA at 20 mg L^{-1} TOC was 82.8%; the $R_{CO_3^{\bullet-}}/R_{total}$ in the presence of mixed NOM at 20 mg L^{-1} TOC was 67.2%; the $R_{CO_3^{\bullet-}}/R_{total}$ in the presence of HA at 20 mg L^{-1} TOC was 51.2%.

Moreover, the different inhibiting effect of different types of NOM may be also asscoiated with the different complexation ability of different types of NOM. It has been reported that NOM tend to combine with nonpolar hydrophobic organic compounds (*e.g.*, dialkyl phthalate (Ogner and Schnitzer, 1970)) via trapping the nonpolar organics in a microscopic hydrophobic environment formed by a micellar or double-layer inner structure or bonding these organics with ionic and hydrogen bonds (Gaffney et al., 1996). In comparison with HA, FA has more carboxylic, phenolic, and ketonic groups which possess ionic and hydrogen bonds and are building blocks of a microscopic hydrophobic inner structure. Therefore, FA may be easier to combine with BPA to form FA-BPA complex in which form BPA is wrapped by FA molecule increasing the steric hindrance for $CO_3^{\bullet-}$/$HO^{\bullet}$ to reach BPA molecules, and thus the degradation of BPA is more inhibited by FA than by HA with Mixed NOM in between.

4. Conclusions

This study focused on the evaluation of the impact of water quality parameters on the formation of reactive radicals and the BPA degradation in the UV/SPC system. The pathways of BPA transformation by $CO_3^{\bullet-}$ were proposed for the first time. The potential of UV/SPC system for wastewater treatment was assessed first with BPA degradation in the secondary effluents collected from a local WWTP and second with the impact of various water quality parameters (*i.e.*, pH, common anions, and NOM) on BPA degradation. Based on the results obtained and the discussion presented, the following conclusions are drawn:

- $CO_3^{\bullet-}$ initiates BPA degradation *via* hydroxylation of the phenolic ring, oxidation demethylation of the isopropylidene group, and homolytic cleavage of the linking bond between isopropylidene and the aromatic ring.
- $CO_3^{\bullet-}$ oxidation can activate the isopropylidene group to accelerate BPA degradation in comparison to direct UV photolysis.
- The increase of pH from 3 to 10.7 decreases the $[HO^{\bullet}]_{ss}$, resulting in a decrease of k_{obs} in both systems.
- The addition of HCO_3^- decreases both $[HO^{\bullet}]_{ss}$ and $[CO_3^{\bullet-}]_{ss}$, leading to a significant decrease of k_{obs} in both systems.
- NOM shows little impact on the formation of $CO_3^{\bullet-}$ while decreases $[HO^{\bullet}]_{ss}$ in the order of FA > mixed NOM > HA causing the corresponding decrease of k_{obs}.

The results from this study provide information on the kinetics and mechanism of BPA transformation in UV/SPC system. The evaluation of the impact of water quality parameters provides insights towards the optimization of UV/SPC system for BPA degradation and gathers more information on the application potential of this system. The data produced in this study are also valuable for computational modelling and prediction of TPs during UV/SPC treatment.

Declaration of Competing Interest

The authors declare that they have no known competing financial interests or personal relationships that could have appeared to influence the work reported in this paper.

Acknowledgements

The author J. Gao would like to acknowledge the International Collaborative Research Project of National Natural Science Foundation of China (51720105001), China Scholarship Council (CSC) scholarship (201406780006), and GSG Research Fellowship awarded by Graduate Student Government at University of Cincinnati, for their financial support. J. Gao also wants to thank Dr. Ningyuan Zhu for his introductory assistance in performing variation partitioning and hierarchical partitioning analysis. The author D. D. Dionysiou acknowledges support from the Herman Schneider Professorship in the College of Engineering and Applied Sciences, University of Cincinnati. The author R. F. Nunes acknowledges the support from the Fulbright Commission in Brazil.

Supplementary materials

Supplementary material associated with this article can be found, in the online version, at doi:10.1016/j.watres.2022.118457.

References

Autin, O., Hart, J., Jarvis, P., MacAdam, J., Parsons, S.A., Jefferson, B., 2013. The impact of background organic matter and alkalinity on the degradation of the pesticide metaldehyde by two advanced oxidation processes: UV/H_2O_2 and UV/TiO_2. Water Res. 47 (6), 2041–2049.

Bodhipaksha, L.C., Sharpless, C.M., Chin, Y.P., MacKay, A.A., 2017. Role of effluent organic matter in the photochemical degradation of compounds of wastewater origin. Water Res. 110, 170–179.

Clara, M., Strenn, B., Saracevic, E., Kreuzinger, N., 2004. Adsorption of bisphenol-A, 17β-estradiole and 17α-ethinylestradiole to sewage sludge. Chemosphere 56 (9), 843–851.

Crain, D.A., Eriksen, M., Iguchi, T., Jobling, S., Laufer, H., LeBlanc, G.A., Guillette, L.J., 2007. An ecological assessment of bisphenol-A: Evidence from comparative biology. Reprod. Toxicol. 24 (2), 225–239.

Fan, C., Horng, C.Y., Li, S.J., 2013. Structural characterization of natural organic matter and its impact on methomyl removal efficiency in Fenton process. Chemosphere 93 (1), 178–183.

Fan, D., Yin, W., Gu, W., Liu, M., Liu, J., Wang, Z., Shi, L., 2021. Occurrence, spatial distribution and risk assessment of high concern endocrine-disrupting chemicals in Jiangsu Province, China. Chemosphere 285, 131396.

Gaffney, J.S., Marley, N.A., Clark, S.B., 1996. Humic and Fulvic Acids. American Chemical Society, pp. 2–16.

Gao, J., Duan, X., O'Shea, K., Dionysiou, D.D, 2020. Degradation and transformation of bisphenol A in UV/sodium percarbonate: Dual role of carbonate radical anion. Water Res. 171, 115394.

Gao, X., Liu, S., Ding, C., Miao, Y., Gao, Z., Li, M., Fan, W., Tang, Z., Mhlambi, N.H., Yan, L., 2021. Comparative effects of genistein and bisphenol A on non-alcoholic fatty liver disease in laying hens. Environ. Pollut. 288, 117795.

Gillam, A.E., Stern, E.S., 1954. An Introduction to Electronic Absorption Spectroscopy In Organic Chemistry. Edward Arnold Publishers.

Goralczyk, K., 2021. A review of the impact of selected anthropogenic chemicals from the group of endocrine disruptors on human health. Toxics 9 (7), 146.

Huang, Y., Kong, M., Westerman, D., Xu, E.G., Coffin, S., Cochran, K.H., Liu, Y., Richardson, S.D., Schlenk, D., Dionysiou, D.D., 2018. Effects of HCO_3^- on degradation of toxic contaminants of emerging concern by UV/NO_3^-. Environ. Sci. Technol. 52 (21), 12697–12707.

Khan, J.A., He, X., Shah, N.S., Khan, H.M., Hapeshi, E., Fatta-Kassinos, D., Dionysiou, D. D., 2014. Kinetic and mechanism investigation on the photochemical degradation of atrazine with activated H_2O_2, $S_2O_8^{2-}$ and HSO_5^-. Chem. Eng. J. 252, 393–403.

Krumova, K., Cosa, G., 2016. Singlet Oxygen: Applications in Biosciences and Nanosciences, Volume 1. Royal Society of Chemistry, pp. 1–21.

Lai, J., Zou, Y., Zhang, J., Peres-Neto, P.R., 2022. Generalizing hierarchical and variation partitioning in multiple regression and canonical analyses using the rdacca. hp R package. Methods in Ecology and Evolution.

Li, S., Hu, J., 2018. Transformation products formation of ciprofloxacin in UVA/LED and UVA/LED/TiO_2 systems: Impact of natural organic matter characteristics. Water Res. 132, 320–330.

Loiselle, S., Vione, D., Minero, C., Maurino, V., Tognazzi, A., Dattilo, A.M., Rossi, C., Bracchini, L., 2012. Chemical and optical phototransformation of dissolved organic matter. Water Res. 46 (10), 3197–3207.

Luo, M., Huang, Y., Zhu, M., Tang, Y.-n., Ren, T., Ren, J., Wang, H., Li, F., 2018. Properties of different natural organic matter influence the adsorption and aggregation behavior of TiO_2 nanoparticles. J. Saudi Chem. Soc. 22 (2), 146–154.

McCabe, A.J., Arnold, W.A., 2017. Reactivity of triplet excited states of dissolved natural organic matter in stormflow from mixed-use watersheds. Environ. Sci. Technol. 51 (17), 9718–9728.

Mercogliano, R., Santonicola, S., Albrizio, S., Ferrante, M.C., 2021. Occurrence of bisphenol A in the milk chain: a monitoring model for risk assessment at a dairy company. J. Dairy Sci. 104 (5), 5125–5132.

Neta, P., Huie, R.E., Ross, A.B., 1988. Rate constants for reactions of inorganic radicals in aqueous solution. J. Phys. Chem. Ref. Data 17 (3), 1027–1284.
Ogner, G., Schnitzer, M., 1970. Humic substances: fulvic acid-dialkyl phthalate complexes and their role in pollution. Science 170 (3955), 317–318.
Parsons, S., 2004. Advanced Oxidation Processes For Water and Wastewater Treatment. IWA Publishing.
Parto, M., Aazami, J., Shamsi, Z., Zamani, A., Savabieasfahani, M., 2021. Determination of bisphenol-A in plastic bottled water in markets of Zanjan, Iran. Int. J. Environ. Sci. Technol. 1–8.
Rosenfeldt, E.J., Linden, K.G., 2004. Degradation of endocrine disrupting chemicals bisphenol A, ethinyl estradiol, and estradiol during UV photolysis and advanced oxidation processes. Environ. Sci. Technol. 38 (20), 5476–5483.
Schmitt, M., Erickson, P.R., McNeill, K., 2017. Triplet-state dissolved organic matter quantum yields and lifetimes from direct observation of aromatic amine oxidation. Environ. Sci. Technol. 51 (22), 13151–13160.
Senra, M.V.X. and Lúcia Fonseca, A. (2021) Toxicological impacts and likely protein targets of bisphenol A in *Paramecium caudatum*. bioRxiv, 2021.2006.2024.449746.
Sharma, P., Chadha, P., 2021. Bisphenol A induced toxicity in blood cells of freshwater fish Channa punctatus after acute exposure. Saudi J. Biol. Sci. 28 (8), 4738–4750.
Staples, C.A., Dorn, P.B., Klecka, G.M., O'Block, S.T., Harris, L.R, 1998. A review of the environmental fate, effects, and exposures of bisphenol A. Chemosphere 36 (10), 2149–2173.
USEPA, 1999. Wastewater Technology Fact Sheet: ultraviolet Disinfection. https://www3.epa.gov/npdes/pubs/uv.pdf.
USEPA, 2010. Bisphenol A Action Plan.
Vandenberg, L.N., Hauser, R., Marcus, M., Olea, N., Welshons, W.V., 2007. Human exposure to bisphenol A (BPA). Reprod. Toxicol. 24 (2), 139–177.
Westall, J.C., Leuenberger, C., Schwarzenbach, R.P., 1985. Influence of pH and ionic strength on the aqueous-nonaqueous distribution of chlorinated phenols. Environ. Sci. Technol. 19 (2), 193–198.